11th World Congress on Computational Mechanics (WCCM XI)
5th European Conference on Computational Mechanics (ECCM V)
6th European Conference on Computational Fluid Dynamics (ECFD VI)
E. Oñate, J. Oliver and A. Huerta (Eds)

# FAILURE OF MULTILAYER COMPOSITES UNDER DYNAMIC LOADING

**SERGEY A. ZELEPUGIN AND ALEKSEY S. ZELEPUGIN**

Physical and Engineering Department
National Research Tomsk State University (TSU)
36 Lenin Avenue, 634050 Tomsk, Russia
e-mail: szel@yandex.ru, www.tsu.ru/english/

Department for Structural Macrokinetics
Tomsk Scientific Center, Siberian Branch, Russian Academy of Sciences (TSC SB RAS)
10/3 Akademicheskii Avenue, 634021 Tomsk, Russia
e-mail: szel@dsm.tsc.ru, www.tsc.ru/en.html

**Key words:** *Failure, Multilayer Composites, Numerical Simulation.*

**Summary.** *The processes of high-velocity interaction of a projectile with a metal-intermetallic laminate (MIL) target were numerically investigated in axisymmetric geometry using the finite element method. To numerically simulate the failure of the material under high velocity impact, we applied the active-type kinetic model determining the growth of microdamages, which continuously changes the properties of the material and induce the relaxation of stresses. The strength characteristics of the medium (shear modulus and dynamic yield strength) depended on temperature and the current level of damage. The critical specific energy of shear deformations was used as a criterion of the erosion failure of the material that occurs in the region of intense interaction and deformation of contacting bodies. To simulate the brittle-like failure of the intermetallic material under high velocity impact, we modified the kinetic model of failure and included the possibility of failure above Hugoniot elastic limit (HEL) in the shock wave and sharp drop in strength characteristics if the failure begins. In the computations, the target consisting from intermetallic* $Al_3Ti$ *- titanium alloy Ti-6-4 layers has been used. The results show that the depth of penetration depends on the thicknesses of intermetallic and titanium alloy layers. The composite target withstands the impact loading in the case of the ratio about 4/1 (*$Al_3Ti$ */ Ti-6-4).*

## 1 INTRODUCTION

The field of material microstructure design targeted for a specific set of structural and functional properties is now a recognized field of focus in materials science and engineering. A new class of structural materials called metal-intermetallic laminate (MIL) composites can have micro-, meso- and macrostructure [1-4]. The superior specific properties of this class of composites makes them attractive for high-performance aerospace applications, and the fabrication method for creating MIL composites allows new embedded technologies to be incorporated into the materials, enhancing their functionality and utility.

In this work the processes of high-velocity interaction of a projectile with a metal-intermetallic laminate target were numerically investigated in axisymmetric geometry using the finite element method. The $Al_3Ti$ – Ti samples were tested on a ballistic stand and the experimental results were presented as well.

## 2 EXPERIMENTAL RESULTS

In the experiments the $Al_3Ti$ – Ti samples were tested on a ballistic stand and the features of the samples failure were investigated. Initial velocity of a hard steel bullet was of 760 m/s.

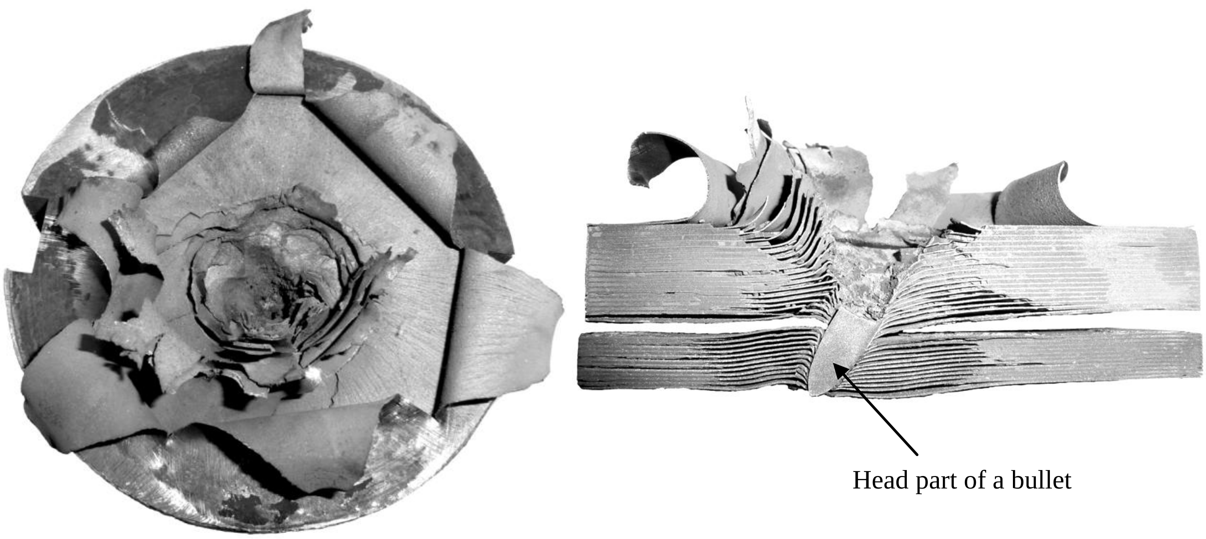


**Figure 1**: Failure of $Al_3Ti$ – Ti sample in ballistic test

In Fig. 1, the $Al_3Ti$ – Ti laminate composite after ballistic test is shown. The measured density of the samples was 3.604 – 3.655 g/cm$^3$. Results of the microanalysis (AT CON,%) for selected points of intermetallic layer: Al = 73.029 - 73.868, Ti = 25.971 - 26.132, which corresponds to $Al_3Ti$ (the density of $Al_3Ti$ is 3.29 g/cm$^3$).

## 3 NUMERICAL SIMULATION

### 3.1 The System of Fundamental Equations

To simulate numerically the processes of high-rate shock loading, we use the model of an elastoplastic damaged medium characterized by the presence of microcavities (pores, cracks). In this model the total volume of the medium W comprises the undamaged part of the medium of density $\rho_c$ which occupies volume $W_c$, and microcavities of zero density which occupy volume $W_f$. The average density of the damaged medium is connected with the above-introduced parameters by the relationship $\rho = \rho_c(W_c/W)$. The degree of damage of the medium is characterized by the specific volume of microcavities $V_f = W_c/(W_*\rho)$.

A mathematical model employed in the numerical code for solving high velocity impact problems is based upon a set of differential equations of continuum mechanics that govern a material flow. The system of equations governing the nonstationary, adiabatic (for both elastic and plastic deformation) motion of a compressible medium with allowance for the evolution of microdamages comprises the continuity equation (1), the equation of motion (2), the energy equation (3), respectively [5-7]:

$$\partial\rho/\partial t + \mathrm{div}\,(\rho v) = 0 \quad (1)$$

$$\rho\, dv_i/dt = \sigma_{ij,j} \quad (2)$$

$$\frac{dE}{dt} = \frac{1}{\rho}\sigma_{ij}\varepsilon_{ij} \quad (3)$$

Here $\rho$ is the density, t is time, $\boldsymbol{\upsilon}$ is the velocity vector, $\upsilon_i$ are the velocity components, $\sigma_{ij} = -P\delta_{ij}+S_{ij}$ are the stress-tensor components, E is the specific internal energy, $\varepsilon_{ij}$ are components of the strain rate tensor, $P = P_c(\rho/\rho_c)$ is the average pressure, $S_{ij}$ are the stress-deviator components, and $P_c$ is the pressure in the continuous component of the medium.

To numerically simulate the failure of the material at high velocity impact, we applied the active-type kinetic model determining the growth of microdamages, which continuously change the properties of the material and induce the relaxation of stresses [8]:

$$\frac{d\,V_f}{d\,t} = \begin{cases} 0,\ \text{if}\ |P_c| \le P^* \text{or if}\ (P_c > P^* \text{and}\ V_f = 0), \\ -\mathrm{sign}(P_c) K_f\,(|P_c| - P^*)(V_2 + V_f), \\ \text{if}\ \ P_c < -P^* \text{or if}\ \ (P_c > P^* \text{and}\ V_f > 0) \end{cases} \quad (4)$$

Here $P^* = P_k V_1/(V_f + V_1)$, and $V_1$, $V_2$, $P_k$, and $K_f$ are material constants determined experimentally. The form of condition (4) was chosen on based on the experimental data. It was assumed that there are fracture nuclei in the material, of identical initial sizes with the effective specific volume $V_1$. Cracks or pores are formed and grow on these nuclei when the stretching pressure exceeds a certain critical value $P^*$ which decreases as formed microdamages grow. The constants in (4) were adjusted by comparing the results of computations and experiments concerning the recording of a free surface velocity when a specimen is loaded by planar impulses of compression. One and the same set of constants is used when calculating both build-up and collapse of cracks and pores (depending on the sign of $P_c$).

The material model includes the equation of state of the Mie-Grüneisen type that represents pressure as a function of specific volume and specific internal energy, the deviatoric elastic constitutive relationships, the von Mises yield criterion taking into account temperature effects. The strength characteristics of the medium (shear modulus and dynamic yield strength) depend on temperature and the current level of damages.

The pressure in the undamaged substance is determined by the Mie-Grüneisen equation of state according to the formula:

$$\begin{aligned} P_c &= \rho_0 a^2 \mu + \rho_0 a^2 \left[1 - \gamma_0/2 + 2(b-1)\right]\mu^2 + \\ &+ \rho_0 a^2 \left[2(1-\gamma_0/2)(b-1) + 3(b-1)^2\right]\mu^3 + \gamma_0 \rho_0 E, \end{aligned} \quad (5)$$

where $\mu = V_0/(V-V_f)-1$, $\gamma_0$ is the Grüneisen coefficient, $V_0$ and V are the initial and current specific volumes, respectively, and a and b are the constants of the Hugoniot shock adiabat described by the relation [9]:

$$u_s = a + b u_p ,$$

where $u_s$ is the shock-wave velocity and $u_p$ is the particle velocity of the substance behind the shock-wave front.

We assume that the change in porosity is influenced only by the spherical stress component or pressure, whereas the components of the stress deviator are bounded by the independent deviatoric yield function:

$$2G\left(\varepsilon_{ij} - \frac{1}{3}\varepsilon_{kk}\delta_{ij}\right) = \frac{dS_{ij}^0}{dt} + \lambda S_{ij}$$

where $dS_{ij}^0 / dt$ is the Jaumann derivative. Parameter $\lambda$ is zero for elastic deformation, and for plastic deformation, is determined from the Mises yield criterion:

$$S_{ij}S_{ij} = \frac{2}{3}\sigma^2$$

Here G is the shear modulus and $\sigma$ is the dynamic yield point. They are determined according to the relationships [6,8,9]:

$$G = G_0 K_T \left(1 + \frac{cP}{(1+\mu)^{1/3}}\right) \frac{V_3}{(V_f + V_3)}$$

$$\sigma = \begin{cases} \sigma_0 K_T \left(1 + \frac{cP}{(1+\mu)^{1/3}}\right)\left(1 - \frac{V_f}{V_4}\right), \text{ if } V_f \le V_4 \\ 0, \text{ if } V_f > V_4 \end{cases}$$

$$K_T = \begin{cases} 1, & \text{if } T_0 \le T \le T_1 \\ \frac{T_m - T}{T_m - T_1}, & \text{if } T_1 < T < T_m \\ 0, & \text{if } T \ge T_m \end{cases}$$

Here $T_m$ is the melting point of the substance, and c, $V_3$, $V_4$, and $T_1$ are the constants.

In the calculations, the function $K_T(T)$ was chosen to model the nonthermal character of plastic deformation and dynamic strength of solids at high strain rates ($10^4$ $sec^{-1}$ or higher) [8].

To calculate the temperature, we used the relations [6]:

$$dT = \begin{cases} d(E - E_{0,c})/c_p, & \text{if } T < T_m \\ 0, & \text{if } T = T_m \\ d(E - E_{0,c} - \Delta H_m)/c_p, & \text{if } T > T_m \end{cases}$$

where the specific heat $c_p$ increases linearly as the temperature increases to the melting point of the substance:

$$c_p = \begin{cases} c_p^0 + \dfrac{c_p^L - c_p^0}{T_m - T_0}(T - T_0), & \text{if } T_0 \le T < T_m \\ c_p^L, & \text{if } T \ge T_m \end{cases}$$

The cold component of the specific internal energy $E_{0,c}$ is given by [9]:

$$E_{0,c} = \begin{cases} E_0, & \text{if } \xi < 0 \\ E_0 + E_1\xi + E_2\xi^2 + E_3\xi^3 + E_4\xi^4, & \text{if } \xi \ge 0 \end{cases}$$

where $\xi = 1 - \rho_0 / \rho_c$, $\Delta H_m$ is the specific heat of melting, $c_p^0$ и $c_p^L$ are material constants,

$$E_0 = -T_0\, c_p^0, \qquad E_1 = \gamma_0 E_0, \qquad E_2 = (a^2 + \gamma_0^2 E_0)/2,$$

$$E_3 = (4ba^2 + \gamma_0^3 E_0)/6, \qquad E_4 = (-2\gamma_0\, ba^2 + 18a^2b^2 + \gamma_0^4 E_0)/24.$$

The critical specific energy of shear deformations is used as a criterion of the erosion failure of the material that occurs in the region of intense interaction and deformation of contacting bodies [10]. The current value of the specific energy of shear deformations is defined from relationship

$$\rho \frac{dE_{sh}}{dt} = S_{ij}\varepsilon_{ij}$$

The critical value of the specific energy of shear deformations depends on the conditions of interactions and is a function of the initial impact velocity

$$E_{sh}^c = a_{sh} + b_{sh}\upsilon_0$$

where $a_{sh}$ and $b_{sh}$ are constants.

When $E_{sh} > E_{sh}^c$ in the computational cell near the contact boundaries, the cell is assumed damaged and the parameters in neighbouring cells are corrected with regard for the principles of conservation laws.

To simulate the brittle-like failure of the intermetallic material under high velocity impact, we modified the kinetic model of failure (4) and included the possibility of failure above HEL in the shock wave and sharp drop in strength characteristics if the failure begins [11].

### 3.2 Numerical results

Computations were carried out by the modified finite element method [12,13]. Sliding conditions were realized between the projectile and target. In the computations, the target consisting from 17 composite intermetallic $Al_3Ti$ - titanium alloy Ti-6-4 layers has been used. Total thickness of the target was 19.89 mm. Thicknesses of intermetallic layer and a layer of titanium alloy were varied. The penetrator used was a tungsten heavy alloy 93W-7FeCo rod with initial diameter of 6.15 mm and length of 23 mm. Initial impact velocity was of 900 m/s.

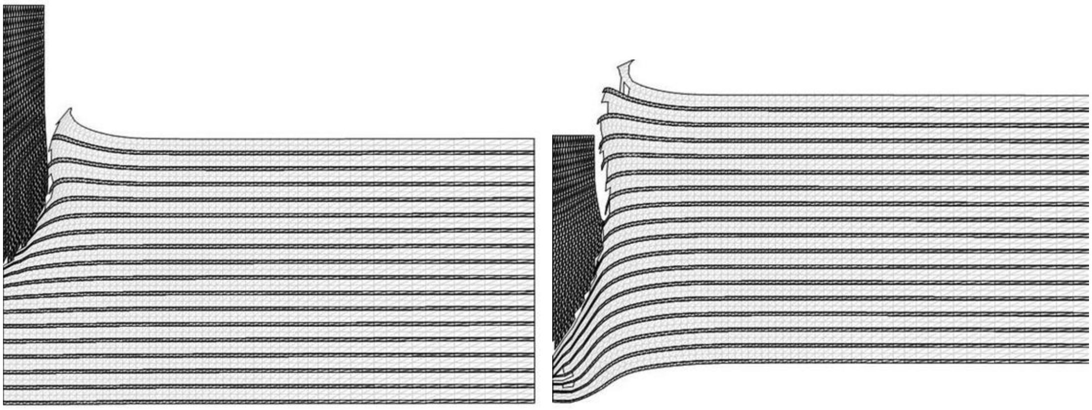

**Figure 2**: Computer images of a radial section of the projectile/target assembly at 15 and 60 μs

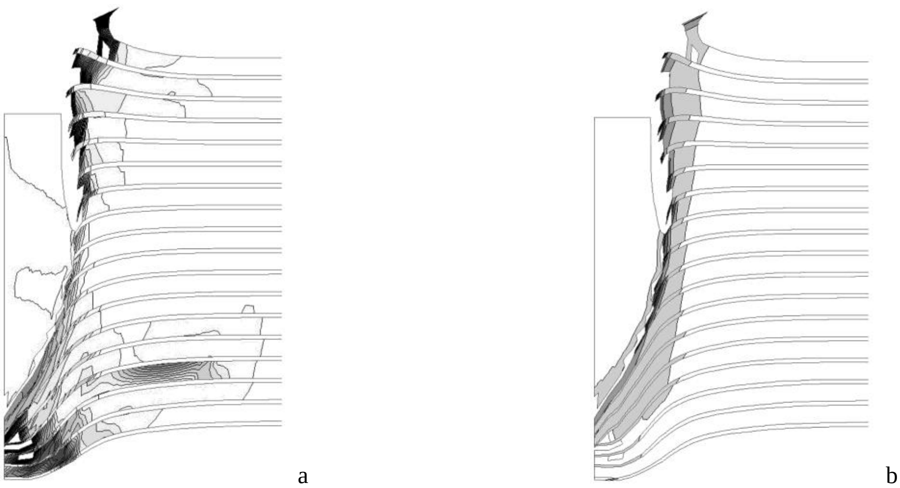


**Figure 3**: Specific volume of microdamage (a) and specific shear deformation energy (b) at 60 μs

Fig. 2 shows computer images of a radial section of the projectile and composite target at the moments of time of 15 and 60 μs. Thickness of intermetallic $Al_3Ti$ layer in this case was of 0.94 mm, thickness of a layer of titanium alloy Ti-6-4 was of 0.23 mm. The computations demonstrate the fact that the MIL composite target withstands the impact loading.

The distribution of the damage and deformation patterns are illustrated in Figs. 3a and 3b, which show the contours of a radial section of the projectile and composite target and contours and fields of the specific volume of microdamage (Fig. 3a) and of the specific shear deformation energy (Fig. 3b). The low level of microdamage in layers of titanium alloy shows the termination of propagation of brittle damage taking place in intermetallic layers.

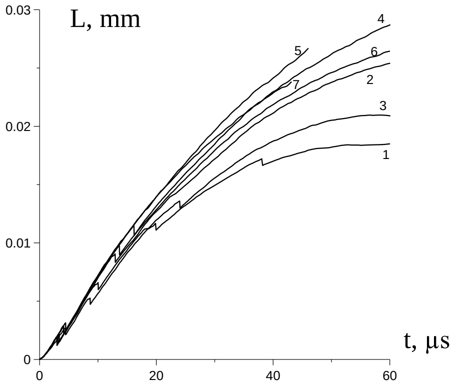


**Figure 4**: Depth of penetration. Numbers of curves correspond to the Table

**Table 1**: Thickness of layer and areal density of the target

| | $Al_3Ti$, mm | Ti-6-4, mm | Areal density, $g/cm^2$ |
|---|---|---|---|
| 1 | 0.94 | 0.23 | 7.02 |
| 2 | 1.17 | - | 6.54 |
| 3 | - | 1.17 | 8.97 |
| 4 | 0.47 | 0.7 | 7.99 |
| 5 | 0.23 | 0.94 | 8.49 |
| 6 | 0.7 | 0.47 | 7.52 |
| 7 | 1.04 | 0.13 | 6.81 |

Fig. 4 illustrates the time dependence of depth of penetration for different targets. The results show that the depth of penetration depends on the thicknesses of intermetallic and titanium alloy layers. The MIL composite target withstands the impact loading in the case of 0.94 mm $Al_3Ti$ / 0.23 mm Ti-6-4 (the ratio is about 4/1). In this case the intermetallic layer provides the failure of the projectile and the metal layer terminates the propagation of damage.

## 4 CONCLUSIONS

- Results obtained demonstrate that destruction of the intermetallic layer is brittle as against to plastic failure of the metal layer.
- It was shown in the computations that the optimal composite target has higher ballistic resistance in comparison with a uniform target either $Al_3Ti$ or Ti-6-4. Optimum construction of the MIL composite should include metal layer of sufficient thickness, which should provide the termination of propagation of brittle damage.
- The results show that the depth of penetration depends on the thicknesses of intermetallic and titanium alloy layers. The composite target withstands the impact loading in the case of the ratio about 4/1 ($Al_3Ti$ / Ti-6-4).

## 5 ACKNOWLEDGEMENTS

We thank A.M. Patselov, V.F. Tolkachev, O.A. Shkoda, O.K. Lepakova for help in conducting the experiments.

The reported study was partially supported by the Russian Foundation for Basic Research (project no. 14-08-31208) and the Ministry of Education and Science of the Russian Federation under contract № 2014/223 (project no. 1943).

## REFERENCES

[1] Vecchio, K.S. Synthetic multifunctional metallic-intermetallic laminate composites. *JOM* (2005) **March**:25-31.

[2] Price, R.D., Jiang, F., Kulin, R.M., and Vecchio, K.S. Effects of ductile phase volume fraction on the mechanical properties of Ti-$Al_3$Ti metal-intermetallic laminate (MIL). *Materials Science and Engineering A* (2011) **528**:3134-3146.

[3] Li, T., Jiang, F., Olevsky, E.A., Vecchio, K.S., and Meyers, M.A. Damage evolution in Ti6Al4V–$Al_3$Ti metal-intermetallic laminate composites. *Materials Science and Engineering A* (2007) **443**:1-15.

[4] Zelepugin, S.A., Mali, V.I., Zelepugin, A.S., and Ilina, E.V. Failure of metallic-intermetallic laminate composites under dynamic loading. *Shock Compression of Condensed Matter*. *USA: American Institute of Physics* (2012) **1426**:1101-1104.

[5] Zelepugin, S.A. and Zelepugin, A.S. Modeling of the destruction of targets during a high-velocity impact. *Russian Journal of Physical Chemistry B* (2008) **2**(2):246-250.

[6] Zelepugin, S.A. and Nikulichev, V.B. Numerical modeling of sulfur – aluminum interaction under shock-wave loading. *Combustion, Explosion, and Shock Waves* (2000) **36**(6):845-850.

[7] Ivanova, O.V., Zelepugin, S.A., Yunoshev, A.S., and Silvestrov, V.V. A multicomponent medium model for reacting porous mixtures under shock wave loading. *J. Energetic Materials* (2010) **28**(1):303-317.

[8] Kanel, G.I., Fortov, V.E., and Razorenov, S.V. Shock waves in condensed-state physics. *Physics-Uspekhi* (2007) **50**(8):771-791.

[9] Gust, W.H. High impact deformation of metal cylinders at elevated temperatures. *J. Appl. Phys.* (1982) **53**(5):3566-3575.

[10] Zelepugin, S.A. Numerical modelling of high-velocity interaction of bodies accounting for the model of erosion-type destruction. *Computational Technologies* (2001) **6**(2):163-167 [in Russian].

[11] Gorelskii, V.A., Zelepugin, S.A., and Tolkachev, V.F. Experimental and numerical study of ceramics destruction by high-velocity impact. *Chemical Physics Reports* (2000) **18**(10-11):2211-2217.

[12] Johnson, G.R. High velocity impact computations in three dimensions. *J. Appl. Mech.* (1977) **44**(1):95-100.

[13] Gorelski, V.A., Zelepugin, S.A., and Smolin, A.Yu. Effect of discretization in calculating three-dimensional problems of high-velocity impact by the finite-element method. *Computational Mathematics and Mathematical Physics* (1997) **37**(6):722-730.